A time domain phase-gradient based ISAR autofocus algorithm

W. Nel*, E. Giusti[+], M. Martorella[+], M.Y Abdul Gaffar*

*Council for Scientific and Industrial Research (CSIR), South Africa, wajnel@csir.co.za
+ University of Pisa, Italy, elisa.giusti@iet.unipi.it

Abstract

Autofocus is a well known required step in ISAR (and SAR) processing to compensate translational motion. This research proposes a time domain autofocus algorithm and discusses its relation to the well known phase gradient autofocus (PGA) technique. Results on simulated and measured data show that the algorithm performs well. Unlike many other ISAR autofocus techniques, the algorithm does not make use of several computationally intensive iterations between the data and image domains as part of the autofocus process. As such, the proposed algorithm could prove to be faster than other techniques. Observations are made regarding the type of phase errors that can be handled, and it is argued that the technique could be posed either as parametric or non-parametric depending on the type of phase errors expected.

Keywords: ISAR, Autofocus, Phase Gradient, Time-Domain.

1. Introduction

To form Inverse Synthetic Aperture Radar (ISAR) imagery the radar imaging system has to compensate for translational motion of the target. Typically, this is done either in a two step approach by performing range alignment and then non-parametric autofocus [1, 4] or by parametric joint range alignment and autofocus algorithms such as in [3].

Most of the parametric techniques model the phase error induced by the motion of the target as a polynomial function of sufficient order (typically allowing for velocity and acceleration error). They then employ image domain measures of image focus (such as contrast or entropy) and recursively estimate the parameters of the model until maximum focus is reached.

Non-parametric approaches often start from the assumption that range aligned high range resolution (HRR) profiles have been generated via some coarse range alignment technique [7, 4]. The autofocus step then estimates the phase-error caused by the translational motion compensation without assuming a model of the target's motion, since the range alignment process can induce higher order errors. Such techniques include Phase gradient autofocus (PGA) [2,6] (developed for focusing of spotlight SAR) and the minimum-variance technique [1].

It is clear that model based approaches are not suited to cases where the phase error does not fit the model chosen [2]. Conversely, non-parametric techniques might not converge in high clutter or very-low SNR conditions. Ideally an 'ISAR toolbox' thus has to contain both approaches.

A common factor between most current autofocus techniques is that the range-Doppler image domain is required to either suppress unwanted interference (e.g. PGA, min-variance) or to measure the quality of the image focus (e.g. ICBA, entropy). Thus, both parametric and non-parametric techniques iterate between the image domain and data domain making them computationally intensive for larger data sets.

This paper develops a range-time domain approach which can either be made parametric or non-parametric. It does not require iteration between the data and imaging domain as the estimation of the translation motion phase-error is carried out completely in the range-time domain. Loosely, the technique can be described as a time-domain phase gradient autofocus approach.

Section 2 describes the system model and provides more detail regarding related work from [1] and [2]. Section 3 then develops the proposed technique.

Section 4 illustrates the performance of the technique on simulated data. It is shown that the proposed technique produces promising results. A discussion provides insight into the type of phase errors that can be compensated, making a case that algorithms which employ separate range-alignment, should use autofocus algorithms that can correct for higher order phase errors, or that use non-parametric phase-compensation, to compensate the tracking errors in the phase induced by the range alignment process.

Section 5 shows examples of results obtained using this technique on measured data, showing also an initial comparison with a dominant scatterer based technique.

Section 6 concludes with suggestions for future research.

2. System model and related work

Assume as input, a signal $s_n(m)$ consisting of M range-aligned HRR profiles with N range bins each. Following the notation and model used in [1], the phase of a (somewhat dominant) scatterer in range bin n can be written as

$$\phi_n(m) = \gamma(m) + 2\pi f_k m + \mu_{0,n} + \rho_n(m) \qquad (1)$$

$\gamma(m)$ denotes the common translational motion phase error, considered range independent. f_k is the Doppler frequency of the scatterer k, and the term $2\pi f_k m$ represents the phase progression of this scatterer over slow time assuming a small angle of rotation over the imaging interval and a fixed rotation rate. $\mu_{0,n}$ is the constant initial phase of the n-th range bin and $\rho_n(m)$ is the phase contribution by other interfering scatterers from the target, clutter or noise.

2.1. PGA and min-variance methods for estimating $\gamma(m)$

To estimate the translational motion compensation factor from $\phi_n(m)$ one has to suppress errors induced by the second, third and fourth terms in Equation (1).

The PGA algorithm [6, 2] and the minimum-variance algorithm [1] both proceed to eliminate the 2nd term, $2\pi f_k m$, by Fourier processing the data to form a set of n Doppler profiles. These profiles are centre shifted such that the

brightest target in each range bin is demodulated to the zero-Doppler bin.

In PGA, the effect of interferers are then minimised via *windowing* of the data in the Doppler domain (equivalent to low pass filtering in the slow-time domain). The complete process ensures that the estimated phase response can be based on an integrated contribution of scatterers over range. Wahl [2] argues that the scatterers need not be dominant and that non-dominant scatterers still capture some information about the characteristics of the phase error.

After an inverse Fourier transforms, the phase $\phi_n(m)$ is estimated by first estimating its gradient and then integrating to obtain an estimate of $\gamma(m)$ as

$$\hat{\gamma}(m) = \sum_{l=2}^{m} \dot{\phi}(m), \hat{\gamma}(1) = 0 \qquad (2)$$

The calculation of the gradient using the complex conjugate reduces the need for phase unwrapping and eliminates the need to estimate $\mu_{0,n}$ since it is eliminated by the phase gradient procedure.

After centre-shifting and windowing, the development of the minimum-variance technique by Bhao et al [1] performs estimation of the phase-error via local phase-unwrapping of $\phi_n(m)$. They proceed to develop a minimum-variance estimator of $\gamma(m)$.

3. Development of the time-domain autofocus approach

From Eq (1) the phase derivative of the response in range bin *n* can be simply calculated as

$$\frac{d\phi_n(m)}{dm} = \dot{\gamma}(m) + 2\pi f_k + 0 + \dot{\rho}_n(m) \qquad (3)$$

Analysing each of the terms we see that (a) the contribution of the initial phase of the range-bin is zero (b) the phase progression of scatterer *k* becomes a constant related to its Doppler frequency f_k and (c) one is left with the derivatives of the clutter/noise contribution $\dot{\rho}_n(m)$ and the translation-phase error $\dot{\gamma}(m)$.

Averaging Equation (3) over N range bins we obtain

$$\overline{\frac{d\phi_n(m)}{dm}} = \overline{\dot{\gamma}(m)} + \frac{2\pi}{N}\sum_{k=1}^{N} f_k + \overline{\dot{\rho}_n(m)} \qquad (4)$$

Now, the first term becomes an estimate of the derivative of the average phase error, since it is independent of range bin *n*. The second term is an estimate of the Doppler centroid of the object being imaged, based on phase contributions (i.e. not weighted by amplitude at all).

It becomes apparent that one can build an estimator of the required translation motion compensation factor based on the integral of Equation (4), if you can reduce the effect of the unwanted clutter (third) term.

The phase gradient calculation eliminates the need for centre shifting each scatterer in the range-Doppler domain, and produces a desired estimate of the Doppler centroid of the target scene, which will help to position the final image at zero-Doppler once compensated.

3.1. Estimating the phase error $\gamma(m)$

Similar to PGA [7], we can form the phase derivative in Equation (3) from phase differences, as

$$\Delta\phi_n(m) \approx \angle(s_n{}^*(m-1)s_n(m)), \Delta\phi_n(1) = 0 \qquad (5)$$

for each *m = 2..M* where M is the number of HRR profiles and $s_n(m)$ is the complex return in the range-time domain. This estimator of the translation motion phase compensation factor based on the phase gradient also has the advantage that it avoids the need for phase unwrapping[1].

To estimate $\gamma(m)$ we proceed by simply building an estimator as

$$\Delta\hat{\gamma}(m) = \frac{1}{R}\sum_{r=1}^{R} \Delta\phi_r(m) \qquad (6)$$

with the mean taken over *r* range bins yet to be determined. It is clear that this estimator will still be affected by the clutter term $\Delta\rho_n(m)$, unless somehow suppressed. Two separate measures are proposed to suppress the effect of the unwanted clutter term.

Firstly, it is proposed (Section 3.2) that the estimation process in Equation (6) should be carried out over a *subset of R selected range bins* which will optimally contribute to suppressing the effect of the clutter.

Secondly, it is proposed (see section 3.3) that the obtained set of values for $\Delta\gamma(m)$ *should be filtered* either by curve fitting (making it parametric) or by low/bandpass filtering in the time domain (allowing for higher order errors to be compensated) or both.

This filtering could be done after the summation over the R selected range bins to make it computationally effective.

3.2 Range bin selection

Multiple scatterer algorithms often make use of amplitude dominance/variance of a range bin as a method to select the subset of range-bins used in phase error estimation. However, amplitude dominance alone is not a guarantee that a particular dominant scatterer adheres to our model.

Amplitude variance, by itself, can be affected by the scattering mechanism, particularly for highly directional scatterers such as flat plates or long dipoles that often dominates the return smaller boats like, sailing yachts, for example.

Thus, it is proposed here rather employ *joint* statistic based on both *phase stability* and *amplitude dominance*.

Since the standard deviation of $\Delta\phi_n(m)$ should be low for a dominant scatterer that fit the range-Doppler imaging model, we can calculate first a statistic which we term the *phase stability*, $\Omega(n)$, from the standard deviation of $\Delta\phi_n(m)$ as shown in Equation (7).

At high SNR, low values of $\hat{\Phi}(n)$ should indicate a stable somewhat dominant scatterer. Conversely, should most of the phase-variance be due to noise, $\hat{\Phi}(n)$ should be approximately equal in all range bins and thus have little influence on range bin selection. Lastly, bins that contain have significant competing clutter will typically not have low phase variance unless the clutter is very point-like.

$$\hat{\Phi}(n) = \left(\frac{1}{M-2}\sum_{m=1}^{M-1}\left(\Delta\phi_n(m) - \overline{\Delta\phi_n(m)}\right)^2\right)^{1/2}$$
$$\Omega(n) = -\hat{\Phi}(n) + \overline{\hat{\Phi}(n)} \qquad (7)$$

[1] The phase derivative should not be calculated as $\angle s_n(m+1) - \angle s_n(m)$ since this will produce phase wrapping errors.

The second step in Equation (7), centres the estimate on its mean, and inverts it, so that small standard deviations will results in local peaks (rather than local minima).

Next, a second statistic based on the average amplitude of the range bin, so as to weight more, those bins with a higher average energy[2] is also formed.

$$A(n) = \sqrt{\overline{|s_n(m)|}} \qquad (7)$$

Finally, the two statistics are combined by multiplication to form a final equally weighted statistic $\Psi(n)$ as

$$\Psi(n) = A(n)\Omega(n) \qquad (8)$$

To select range bins, we find the local maxima of $\Psi(n)$ that exceed a fixed threshold. The threshold is typically set at 20% of the maximum of $\Psi(n)$.

In practice, for ISAR imaging of small sea vessels, it has been found that the selection approach described above, can prevent the selection of weaker, clutter only, range bins, which will otherwise play a significant role in the phase-error estimation process. A more optimal weighting between phase stability and amplitude contribution is a topic for further study.

3.3. Options for filtering the estimate $\Delta\hat{\gamma}(m)$

To further reduce the effect of unwanted clutter/noise, it is proposed that either a low-pass filter or a parametric fit is used to smooth the estimate of $\Delta\hat{\gamma}(m)$. The choice of technique here will depend on the expected characteristics of the phase-error term.

Note that it is possible to iterate the algorithm, since, in each iteration either the model order or filter bandwidth can be reduced (similar to PGA) resulting in a better estimate of the derivative of the residual phase error. The magnitude of the phase error estimate can be monitored to determine convergence.

4. Simulation Results

Simulation results were produced to highlight some of the steps of the proposed algorithm. The simulation is based on a stepped FM radar model to produce HRR profiles, at X Band with 600MHz bandwidth and 10 MHz steps. 20 scatterers with varying amplitudes and positions are simulated to form a target with dimensions ≈ 5m x 2m x 5m. For purpose of illustration SNR is set rather high at about 30dB (after HRR profiling). In general, the algorithm performs well in worse SNR conditions, as seen in measured data.

The translational motion of the target is simulated to be third order with R_0=10km, v_0=5m/s,a_0= -3m/s^2 and j_0=-2 m/s^3.

The jerk term is specifically included to simulate a small boat at sea undergoing jerk when hit by an ocean wave. The translational motion in this data is rather severe, showing the ability of the algorithm to handle severe phase errors, typically not handled by 2nd order model based approaches.

Figure 1 shows the aligned range profiles after correlation based range alignment. For this particular case an adapted two pass correlation method is used to perform the range alignment.

Figure 2 shows the range-Doppler image obtained without any autofocus, which is unfocused as expected.

[2] The mean is over M range profiles producing 1 value per range bin.

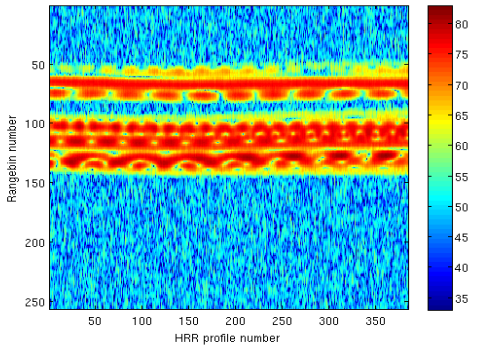

Fig 1. Input range profiles after range alignment.

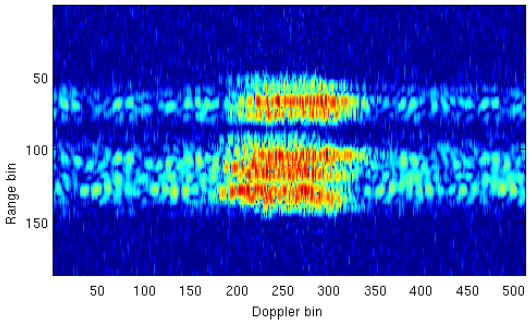

Fig 2. Uncompensated range-Doppler image

Figure 3 shows the statistic $\Psi(n)$ as an estimate of the most phase stable scatterers. Also indicated (in red) are the selected bins for inclusion in the phase estimation process.

Figure 4 shows the resultant phase function and the estimation of the phase error with a low order, zero group-delay low-pass filter.

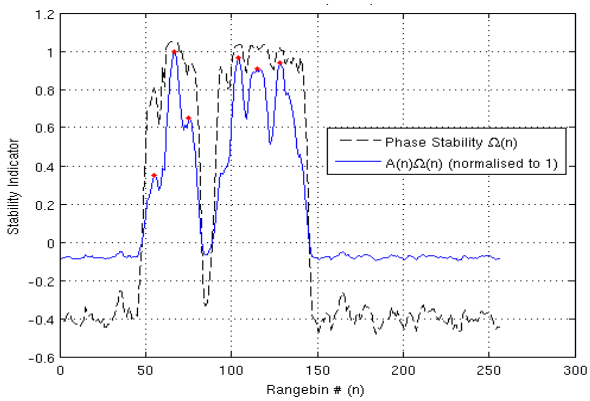

Fig 3. Estimated statistic of the phase stability, and selected range bins to use for phase error estimation.

Although the motion of the simulated target was 3rd order it is clear that the phase error is even higher order. This is most likely induced by range alignment error. Clearly, one should not apply 2nd order polynomial based autofocus algorithms to such range aligned input data.

For the first iteration of the proposed algorithm therefore a filter based approach is used to estimate the phase error. This filter could be designed automatically by analysing the frequency content of the estimated phase error vector.

Figure 5 shows the image after a first step of autofocus. Analysing the phase error at this point reveals a small residual low-frequency error. From practical results it has been seen that a second iteration of the algorithm with this error re-

estimated from a low-order polynomial typically removes the significant remaining phase error in the data.

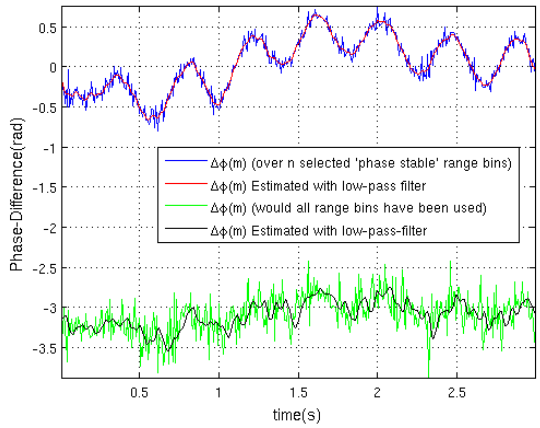

Fig 4. Phase error estimated (red) on first iteration using a low-pass filter. In green the effect of not having chosen any stable scatterers can be seen. *For clarity, the green plot is offset artificially by –π.*

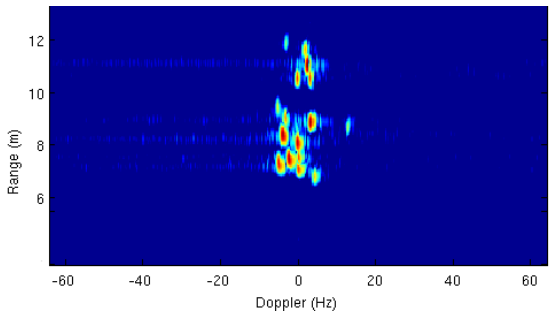

Fig 5. Autofocused image after first iteration. A low-pass filter was used to estimate error.

This second iteration is akin to that of PGA, where window size is decreased to control the filter bandwidth. In the time domain approach a filter with a lower bandwidth can also be realised via a curve fit, resulting in a model based estimate rather than a filter.

4. Results on measured data

Figure 6 shows an ISAR image produced with measurements of a small sailing yacht. The data was captured as part of a trial by CSIR in October 2010. The image using the proposed technique (middle) clearly has a sharp focus on the deck level scatterers, whilst the mast is somewhat blurred when compared with a dominant scatterer algorithm (DSA). As with the simulated data, it is evident that the autofocus technique is effective on measured data. A further comparison is shown in Figure 7, where a plot is made of the image contrast, as a measure of focus, of a series of images taken from this dataset. In this particular case, the proposed algorithm outperforms DSA in about 70% of the cases.

In the other 30%, DSA probably focuses a scatterer that better approximates the high frequency phase errors. These scatterers will not be focused by the proposed technique due to the low-pass filtering on the phase derivative. The issue of adaptive design of this filter clearly requires future research.

5. Conclusions

The proposed time domain phased gradient based autofocus algorithm shows promise, and could be a useful addition to the ISAR specialists' toolbox. In particular, it is believed that efficient implementations of this algorithm can be made, since it does not require several steps of FFT based iterations. Future work should analyse the technique on more data (possibly also spot-SAR) and research optimal ways of choosing the filter bandwidth and scatterer selection statistics.

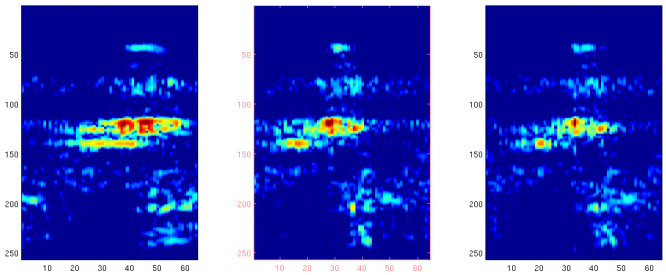

Fig 6. ISAR image of small yacht; (left) Unfocused, (middle) focused using proposed algorithm, (right) focused using DSA.

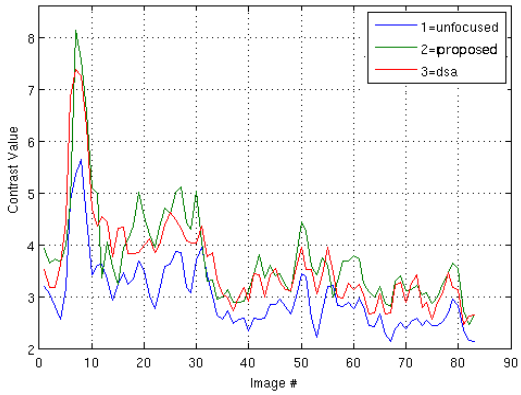

Fig 7. Image contrast comparison of proposed technique, unfocused data and DSA.

Acknowledgements

The authors would like to acknowledge the CSIR AwareNet project that has supported the ISAR research effort at the CSIR, as well as the many people involved in obtaining the datasets used to produce insights and results in the field of ISAR.

References

[1] W. Ye, T. Yeo, Z. Bao, "Weighted Least-Squares Estimation of Phase Errors for SAR/ISAR Autofocus", IEEE Transactions on Geoscience and Remote Sensing, pp. 2487, vol. 37, Sep 1999

[2] D. Wahl, P.H. Eichel, D.C. Ghiglia, C.V. Jakowatz (Jr), "Phase Gradient Autofocus - A Robust Tool for High Resolution SAR Phase Correction", IEEE Transactions on Aerospace and Electronic Systems, pp. 827, vol. 30, no. 3, Jul 1994.

[3] M. Martorella, F. Berizzi, B. Haywood, "Contrast maximisation based technique for 2-D ISAR autofocusing", IEE Radar, Sonar and Navigation Proceedings, pp. 253, vol. 152, no. 4, Aug 2005

[4] T. Itoh, H. Sueda, "Motion Compensation for ISAR Via Centroid Tracking", IEEE Transaction on Aerospace and Electronic systems, pp. 1196, vol. 32, no.3, Jul 1996.

[5] J. Li, R. Wu, V. Chen, "Robust Autofocus Algorithm for ISAR Imaging of Moving Targets", IEEE Transactions on Aerospace and Electronic systems, pp. 1056, vol. 37, no. 3, Jul 2001

[6] C.V. Jakowatz, D.E. Wahl, et al, "Spotlight-mode synthetic aperture radar: A signal processing approach", Kluwer academic publishers.

[7] "Extended envelope correlation for range bin alignment in ISAR", J. M. Muñoz-Ferreras, F. Pérez-Martínez,